10-2-2018

Donor–Acceptor Fluorophores for Energy-Transfer-Mediated Photocatalysis

Jingzhi Lu
University of Nebraska – Lincoln

Brian Pattengale
Marquette University

Qiuhua Liu
University of Nebraska – Lincoln

Sizhuo Yang
Marquette University

Wenxiong Shi
Nanyang Technological University, Singapore

See next page for additional authors

Journal of the American Chemical Society, Vol. 140, No. 42 (October 2, 2018): 13719-13725. DOI.

Donor–Acceptor Fluorophores for Energy-Transfer-Mediated Photocatalysis

Jingzhi Lu
Department of Chemistry, University of Nebraska−Lincoln, Lincoln, Nebraska
Brian Pattengale
Department of Chemistry, Marquette University, Milwaukee, Wisconsin
Qiuhua Liu
Department of Chemistry, University of Nebraska−Lincoln, Lincoln, Nebraska
Sizhuo Yang
Department of Chemistry, Marquette University, Milwaukee, Wisconsin
Wenxiong Shi
School of Materials Science and Engineering, Nanyang Technological University, Singapore 639798, Singapore
Shuzhou Li
School of Materials Science and Engineering, Nanyang Technological University, Singapore 639798, Singapore
Jier Huang
Department of Chemistry, Marquette University, Milwaukee, Wisconsin

Jian Zhang
Department of Chemistry, University of Nebraska−Lincoln, Lincoln, Nebraska

Abtract

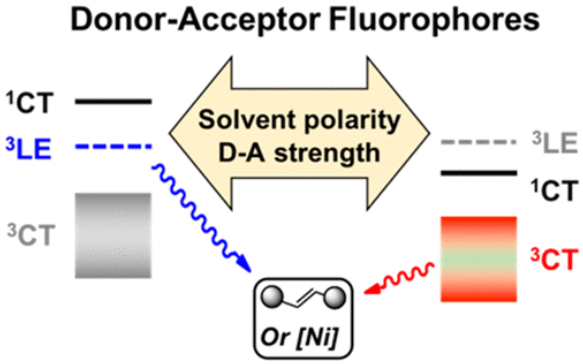

In this work, we report the mechanistic origins of the triplet excited state of carbazole-cyanobenzene donor–acceptor (D–A) fluorophores in EnT-based photocatalytic reactions and demonstrate the key factors that control the accessibility of the ^{3}LE (locally excited triplet state) and ^{3}CT (charge-transfer triplet state) via a combined photochemical and transient absorption spectroscopic study. We found that the energy order between ^{1}CT (charge transfer singlet state) and ^{3}LE dictates the accessibility of ^{3}LE/^{3}CT for EnT, which can be effectively engineered by varying solvent polarity and D–A character to depopulate ^{3}LE and facilitate EnT from the chemically more tunable ^{3}CT state for photosensitization. Following the above design principle, a new D–A fluorophore with strong D–A character and weak redox potential is identified, which exhibits high efficiency for Ni(II)-catalyzed cross-coupling of carboxylic acids and aryl halides with a wide substrate scope and high selectivity. Our results not only provide key fundamental insight on the EnT mechanism of D–A fluorophores but also establish its wide utility in EnT-mediated photocatalytic reactions.

Introduction

The past decade has witnessed a renaissance of photocatalysis in synthetic organic chemistry.(1) Through visible light sensitization, small molecules are activated under mild conditions with high tolerance to functional groups. One popular activation strategy is photoredox catalysis, by which the photocatalyst (PC, also referred to as photosensitizer), upon visible light excitation, initializes two sequential single electron transfer (ET) processes to turn over and promote the transformation of reactant(s) to product(s).(2) A second fundamental activation pathway that does not involve any charge separation is energy transfer (EnT), which occurs directly from the electronically excited state (ES) of PC (*PC) to the substrate and initializes its subsequent transformation.(3) Building on the early studies,(4) the reaction scope of EnT-mediated photocatalysis has been recently expanded to cycloaddition,(5) isomerization,(6) and cross-coupling,(7) to name a few. In several cases, the combination of EnT with other activation modes such as Lewis acid(8) and hydrogen-bond(9) catalysis can also realize excellent enantioselectivity.

One important character for a good PC, regardless the activation pathways, is a sufficiently long-lived ES, which is usually enabled by spin interconversion. While a near unity of Φ_{ISC} (ISC = intersystem crossing) can be often achieved when heavy transition metals (e.g., Ru or Ir) are incorporated in PCs,(10) this strategy induces concerns of potential metal contamination. As a result, metal-free organic PCs that can achieve efficient ISC have become the most attractive alternatives.(11) Organic PCs with high Φ_{ISC} have been reported after incorporating carbonyls and heavy halogens(12) and have been used in synthetic photochemistry for EnT-based reactions.(13) Very recently, we have also developed metal-free PCs based on donor–acceptor (D–A) fluorophores for organic synthesis.(14) The rationale is inspired by the common design principle in thermally assisted delayed fluorescence (TADF), where a sterically hindered D–A dyad usually exhibits a small singlet (^{1}S)–triplet (^{3}T) energy gap (ΔE_{ST}) that increases both down-conversion and up-conversion ISC.(15)

While these examples demonstrate the large potentials of using D–A fluorophores as metal-free PCs for EnT-mediated organic synthesis, the mechanistic origins of the EnT process remain unclear. Typically, the triplet state (^{3}T) of organic D–A fluorophores has two main characters, namely, local excitation (^{3}LE) within a particular molecular subunit (either D or A) and charge-transfer (^{3}CT) transition from the donor-based HOMO to the acceptor-based LUMO. Recent experimental(16) and theoretical(17) studies have revealed that ^{3}LE mediates the efficient ISC from ^{1}CT to ^{3}CT via spin–orbit(18) as well as spin–vibronic coupling.(19) It then raises a question whether both ^{3}CT and ^{3}LE can be utilized for EnT. If so, how can one modulate their accessibility for the synthetic purpose?

Herein, we report a systematic study of the photocatalytic applications of Cz–CN (Cz = carbazole, CN = cyanobenzene)-based D–A fluorophores. Using the well-known *Z*/*E* isomerization of stilbene as a prototypic reaction and optical femtosecond (fs-TA) and nanosecond (ns-TA) transient absorption spectroscopy, we found that indeed both ^{3}LE and ^{3}CT are amenable for the EnT-based reactions, and the energy order between ^{1}CT and ^{3}LE dictates their accessibility. Since the energy level of ^{3}LE is relatively fixed and not significantly affected by reaction media, the tunability of D–A fluorophores is best realized via adjusting the energy level of ^{3}CT, and its accessibility can be achieved by decreasing solvent polarity or increasing the D–A CT character of the fluorophores. Finally, the validity of this design principle was further tested and applied in the identification of new D–A PCs for Ni(II)-catalyzed cross-coupling of carboxylic acids with aryl halides.

Results and Discussion

We chose 11 Cz–CN-based D–A fluorophores of which the number and position of donor and acceptor are systematically changed, including five benzonitrile (BN) derivatives where the BN

core is coupled with two, three (×2), four, and five Cz, as well as six dicyanobenzene derivatives where two and four Cz are coupled with terephthalonitrile (TPN), phthalonitrile (PN), and isophthalonitrile (IPN), respectively (Scheme 1). Except 3,5-2CzBN, most Cz–CN fluorophores exhibit appreciable visible light absorption (>380 nm, see Supporting Information, Figure S1), indicating the generality of D–A fluorophores for visible light photocatalysis. The CT nature of ES of D–A fluorophores was clearly indicated by the sensitive solvatochromism in fluorescence spectra (Figure S2): the more polar solvent dimethylformamide (DMF) results in a larger Stokes shift than the less polar solvent toluene due to the stronger interaction between the CT nature of PC and the dipole of polar solvents, consistent with previous observations.(20) Moreover, as the D–A interaction increases by increasing the number of either Cz or CN, both absorption and emission peaks are red-shifted (Figure S2).

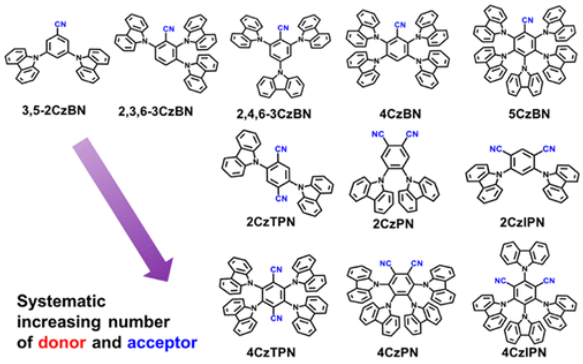

Scheme 1. Chemical Structures of Cz–CN Donor–Acceptor (D–A) Fluorophores Used in This Study

Photosensitized *E*/*Z* isomerization of stilbene was used to evaluate the performance of D–A fluorophores (Figure 1a).(21) This energetically uphill reaction is based on different triplet–triplet EnT efficiency of PC to the two isomers. In general, if the triplet energy (E_T) of PC is smaller than that of the *Z*-isomer but larger than that of the *E*-isomer, EnT is more thermodynamically favorable to the *E*-isomer, resulting in accumulation of *Z*-isomer and a higher *E*/*Z* isomerization efficiency (defined by *Z*/*E* ratio). Provided that the "photostationary state" is reached by sufficient light irradiation, the other photophysical properties of PCs such as molar absorptivity and quantum yield become insignificant. As such, it is convenient to benchmark the photocatalytic efficiencies solely on the basis of E_T.

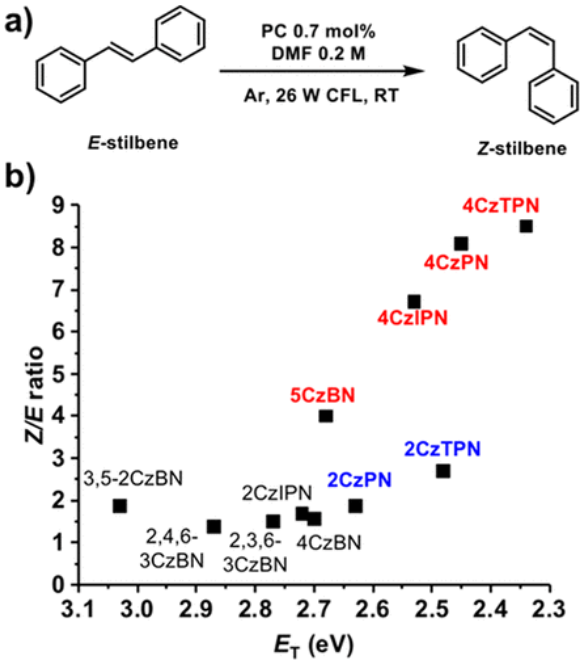

Figure 1. (a) Photosensitized *E*/*Z* isomerization of stilbene. (b) *Z*/*E* ratio at the photostationary state vs E_T of D–A fluorophores.

The isomerization reaction was conducted in a DMF solution of *E*-stilbene (0.2 M) and PC (0.7 mol %) using white light irradiation (26 W compact fluorescence lamp, CFL) under an argon atmosphere at room temperature (Figure 1a). Figure 1b illustrates the correlation between the *Z*/*E* ratio and the energy of the lowest triplet state (E_T, see Supporting InformationTable S3 for details). In general, D–A fluorophores with a large E_T (>2.7 eV) result in lower *Z*/*E* ratios. Specifically, with an E_T of 2.34 eV, which is larger than the E_T of *E*-stilbene (2.2 eV(22)) but smaller than the E_T of *Z*-stilbene (2.5 eV(22)), 4CzTPN shows the highest isomerization efficiency (*Z*/*E* = 8.5), which is followed by 4CzPN (E_T = 2.45 eV, *Z*/*E* = 8.1), 4CzIPN (E_T = 2.53 eV, *Z*/*E* = 6.7), and 5CzBN (E_T = 2.68 eV, *Z*/*E* = 4.0). However, 2CzPN (E_T = 2.63 eV) and 2CzTPN (E_T = 2.48 eV) do not follow the trend and give essentially the same efficiency (*Z*/*E* ≈ 2) as those with a large E_T (Figure 1b).

This deviation prompts us to hypothesize that, in certain D–A fluorophores, instead of the lowest triplet state ($^3T_1$, presumably ^{3}CT), triplet state(s) with a larger energy (^3T_n), likely with a strong ^{3}LE character, are involved in EnT. Indeed, time-dependent density functional theory (TD-DFT) calculations with the UB3LYP functional and 6-31G(d) basis functions have revealed the strong ^{3}LE character of the triplet states of 2CzPN ($^3T_{3-4}$, 3.00–3.05 eV) and 2CzTPN ($^3T_{5-7}$, 3.01–3.18 eV) (see Supporting Information S-7 for detailed computational procedure and results). This hypothesis is also consistent with the pivotal role of ^3T_n with ^{3}LE character in the TADF process by inducing an efficient ISC via spin–orbit coupling.(18) Nevertheless, the EnT from ^{3}LE needs to be experimentally confirmed.

Femtosecond and Nanosecond Transient Absorption Spectroscopy

In order to seek further support for the proposed EnT mechanisms, we turn to fs-TA and ns-TA spectroscopy to investigate the ES dynamics of two model D–A fluorophores, 2CzPN and 4CzIPN, since their ^{3}CT and ^{3}LE states have distinct spectral features.(23) Upon excitation at 400 nm, the fs-TA spectra of both compounds show a prominent absorption band at 480 nm and a broad absorption at >600 nm (Figure 2a and b) that can be assigned to ^{1}CT absorption. At early time (<2 ps) (insets of Figure 2a and b), spectral evolution in the whole spectral window involves the rising of the 480 nm band and decay of the >600 nm absorption feature, which can be attributed to the vibrational cooling from a Franck–Condon (FC) state to the relaxed S_1 state. At later times (>2 ps), distinct growth in the ∼525–700 nm and simultaneous decay at 480 and >700 nm can be attributed to the ISC process from ^{1}CT to the triplet states (^{3}CT/^{3}LE). This evolution agrees well with the ns-TA spectra (Figure 2c and d), where the ISC process continues to evolve until ∼150 ns. Following the ISC process, the triplet states eventually return to the ground state with a slow time constant on a microsecond time scale. The ISC process is further supported by the ns-TA spectra at the NIR region (Figure 2c and d), where the decay of absorption feature at <1000 nm corresponding to ^{1}CT is accompanied by the growth of the feature at >1000 nm that represents the triplet state. According to a previous report, we can further assign the spectral features at 525–700 nm and 900–1200 nm to ^{3}LE and ^{3}CT, respectively.(23) These results together suggest that ^{3}LE and ^{3}CT are both present in 2CzPN and 4CzIPN, and the proposed triplet state (T_1) is likely associated with the equilibrium between ^{3}LE and ^{3}CT.

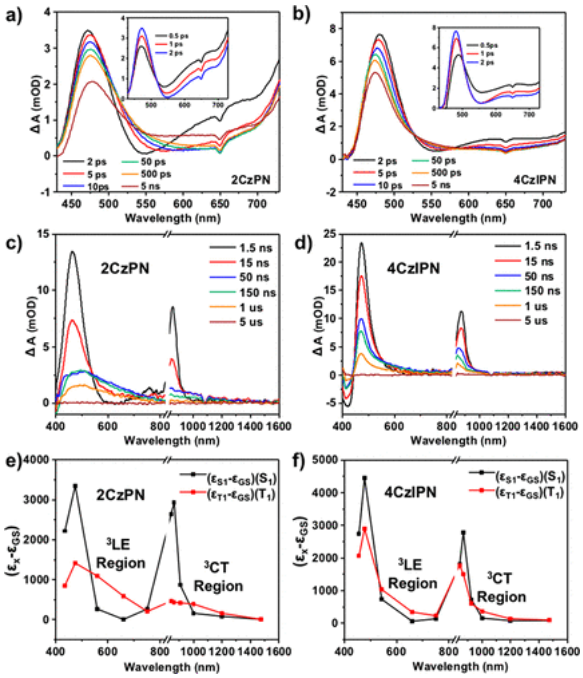

Figure 2. Femtosecond TA spectra of 2CzPN (a) and 4CzIPN (b) in the visible region following 400 nm excitation. The inset shows the corresponding early time spectra. Nanosecond TA spectra of 2CzPN (c) and 4CzIPN (d) in both visible and NIR

regions following 400 nm excitation. The break denotes the spectral range not covered by ns-TA experiments. The extinction coefficients obtained from a global fitting model for 2CzPN (e) and 4CzIPN (f).

We next probe the kinetics of the spectral features of ^{3}LE and ^{3}CT to evaluate the EnT process in the presence of *E*-stilbene as the energy acceptor (quencher). Figure 3 compares the kinetic traces of 2CzPN and 4CzIPN at 660 nm (^{3}LE) and 1000 nm (^{3}CT) in the presence of different concentrations of *E*-stilbene (see Figures S8–S10 in the Supporting Information for TA spectra). The significantly enhanced decay observed for both samples at ^{3}LE and ^{3}CT spectral regions in the presence of *E*-stilbene suggests that both triplet states are responsible for the EnT process, supporting the triple state EnT mechanism, although their relative contribution might be different between 2CzPN and 4CzIPN.

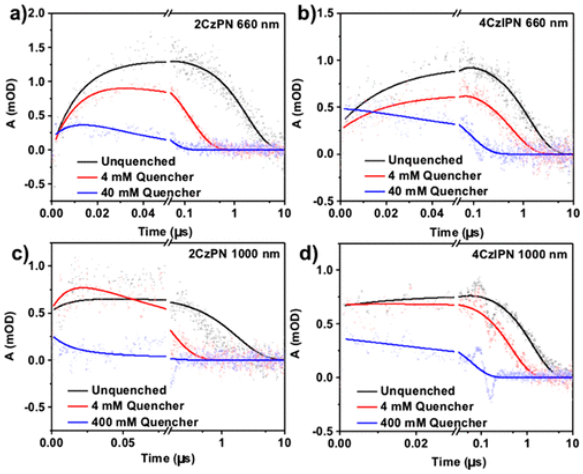

Figure 3. Kinetic traces of ns-TA spectra in the presence of different concentrations of *E*-stilbene (quencher) for 2CzPN at 660 nm (a) and 1000 nm (c) and for 4CzIPN at 660 nm (b) and 1000 nm (d).

To quantitatively evaluate EnT dynamics in these systems, global fitting is used to simultaneously fit the kinetic traces of fs- and ns-TA spectra at different wavelengths by using the same set of rate constants while varying the extinction coefficients (see Supporting Information S-8 for details). We first fit the kinetic traces of the samples in the absence of *E*-stilbene to obtain the time constants for intrinsic ES relaxation dynamics of 2CzPN and 4CzIPN. The best fits to these kinetic traces are shown in Figures S11 and S12. The resulting fitting parameters are listed in Table1, from which we obtained the intrinsic time constants for vibrational cooling ($\tau_1 = 1/k_1$), the ISC process ($\tau_2 = 1/k_2$), and the triplet state lifetime ($\tau_3 = 1/k_3$) for 2CzPN and 4CzIPN. More importantly, we found that the extinction coefficients of S_1 and T_1 obtained from global fitting show excellent agreement with the corresponding ns-TA spectra (Figure 2e and f), which unambiguously confirms the validity of the fitting model.

Table 1. Fitting Parameters for 2CzPN and 4CzIPN Obtained from Global Fitting

sample	[*E*-stilbene]	$\tau_1(ps)$	$\tau_2(ps)$	τ_3 *or* $\tau_{3'}$ (μs)	τ_{EnT}, ^3CT (ns)	τ_{EnT}, ^3LE (ns)
	0 mM			1.8	NANA	
	4 mM			0.132, 0.127	142	137
2CzPN		1.7	25			
	40 mM			0.25	Not measured	25
	400 mM			0.081	85	Not mesured
	0 mM			1.4	NA	NA
	4 mM			0.461, 0.600	687	1050
4CzIPN		5.7	47			
	40 mM			0.176	Not measured	80
	400 mM			0.049	51	Not measured

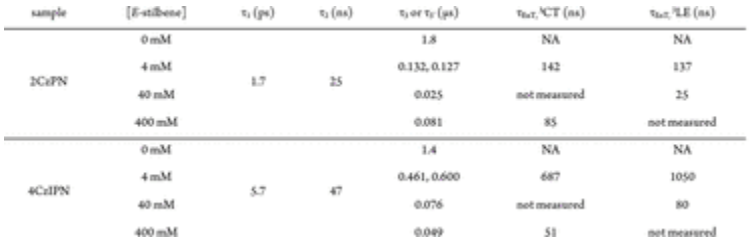

The same model was used to fit the kinetic traces of the TA results in the presence of *E*-stilbene (Figures S13–S15). Because triplet EnT to *E*-stilbene has a negligible effect on the time constants of vibrational cooling (τ_1) and the ISC process (τ_2), these parameters were fixed during the fitting process. The resulting time constant representing the new lifetime of the triplet state in the presence of different concentrations of quencher ($\tau_{3'}$) is also listed in Table1, from which the EnT time constant (τ_{EnT}) was obtained according to $1/\tau_{3'} = 1/\tau_{EnT} + 1/\tau_3$. It is interesting to note that, for 2CzPN, τ_{EnT} from ^{3}LE is slightly shorter than from ^{3}CT in the presence of low concentrations of quencher (4 mM) but much shorter in the presence of higher concentrations of quencher ($\tau_{EnT}(^3LE)$ = 25 ns with 40 mM quencher; $\tau_{EnT}(^3CT)$ = 85 ns with 400 mM quencher). These results suggest that the EnT process is more efficient from ^{3}LE than from ^{3}CT in 2CzPN, although both triplet states contribute to EnT. On the other hand, 4CzIPN shows significantly shorter τ_{EnT} from ^{3}CT than ^{3}LE even at low quencher concentration (4 mM), which indicates that the EnT process is dominated by ^{3}CT in 4CzIPN.

Changing Photophysical Properties of PC to Modulate the EnT Pathway

The mechanistic study highlights the importance of the depopulation of ^{3}LE for using highly tunable ^{3}CT of D–A fluorophores in EnT-based photocatalytic reactions. We envision that when ^{1}CT is lowered, the population of ^{3}LE should become less efficient. Since for most Cz-CN D–A fluorophores the ^{3}LE state usually has a fairly constant value of ~3.1 eV,(23) two strategies

can be used herein to tune the energy level of ^{1}CT and modulate the ^{3}LE/^{3}CT population. (1) Changing solvent polarity. Since the absorption of Cz-CN D–A fluorophores usually red-shifts in less polar solvents (Figure S2), changing solvent polarity may serve as an approach to modulate the ^{3}LE/^{3}CT population. Indeed, for 2CzTPN, we observed an increase of *Z*/*E* ratio from 2.7 in DMF to 7.3 in toluene. The red-shift of the UV–vis spectra of 2CzTPN in toluene is comparable with that in DMF (Figure 4a), via which the lowest-energy absorption band ($^1CT_{abs}$, based on the peak position) becomes lower than ^{3}LE and causes the depopulation of the latter. (2) Increasing D–A CT character. An increase of the donor strength in D–A fluorophores is another strategy to increase the CT character and decrease the ^{1}CT energy. For instance, although changing the solvent polarity for 2CzPN only results in a limited difference of *Z*/*E* ratio in DMF (1.9) and toluene (2.1), which is consistent with its $^1CT_{abs}$ being at a larger energy than ^{3}LE in both solvents, replacing Cz with a stronger donor, such as 3,6-di-*tert*-butylcarbazoyl– (^{t}BuCz, E_T = 2.97 eV(24)), shifts $^1CT_{abs}$ below ^{3}LE and increases the *Z*/*E* ratio to 4.6 (in toluene) in accordance with ^{3}CT energy of 2tBuCzPN (~2.56 eV(25)) (Figure 4b). Overall, both experiments strongly suggest that tuning the energy of ^{1}CT can effectively modulate the ^{3}LE/^{3}CT population and dramatically vary the photocatalytic efficiency of the *Z*/*E* isomerization of stilbene. In fact, upon switching solvent and increasing donor strength, the new *Z*/*E* ratios exhibit a good correlation with the E_T values, suggesting the population of ^{3}CT and corresponding enhanced EnT (Figure S3).

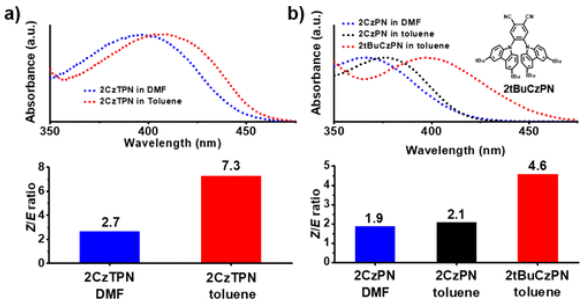

Figure 4. Fine-tuning the $^1CT_{abs}$ energy level to increase *E*/*Z* isomerization of stilbene by (a) changing solvent polarity and (b) increasing the D–A CT character.

On the basis of the mechanistic understanding of the EnT process, we next further demonstrate the utility of D–A fluorophores for other photoisomerization reactions that have different energetic requirements. As for β-methylstyrene with an E_T of the *Z*- and *E*-isomer of 2.9 and 2.6 eV, respectively,(26) 5CzBN, which has an E_T of 2.68 eV, would be an optimal PC. To our delight, 5CzBN indeed gave rise to the highest *Z*/*E* ratio of 7.3 in DMF among the four D–A fluorophores exhibiting a dominant ^{3}CT character (Table S7). Such catalytic activity is comparable to Ir(ppy)$_3$ (ppy = 2-phenylpyridine, E_T = 2.51 eV)(6a) and much more efficient than conventional organic photosensitizers including benzophenone, benzil, and 9-fluorinone (Table S8). Similar results were found in the *Z*/*E* isomerization of diisopropyl fumarate (E_T = 2.7 eV) to

maleate (E_T = 3.1 eV);(27) 5CzBN gave an excellent *Z*/*E* ratio of 32 in DMF, outperforming Ir(dF-CF_3-ppy)$_2$(dtbpy)PF_6 (*Z*/*E* ratio = 7.3, E_T = 2.64 eV(28)) (Table S9). As expected, 4CzIPN is ineffective due to its lower E_T.

EnT-Promoted Cross-Coupling of Carboxylic Acids and Aryl Halides via Nickel Complexes

We anticipate the design principle of D–A fluorophores can also be applied for other EnT-mediated reactions where the organometallic complex is the acceptor. MacMillan and co-workers recently reported the cross-coupling between carboxylic acids and aryl halides promoted by Ir(ppy)$_3$ via EnT to a nickel(II)-based catalyst.(7b) We predicted that a D–A fluorophore with an E_T larger than that of Ir(ppy)$_3$ (2.33 eV) should provide a sufficient sensitization efficiency. 4CzIPN was first elected as the PC due to its appropriate E_T value (2.53 eV) and good compatibility with Ni(II) complexes in ET-based reactions.(14b) The reaction of benzoic acid (**1**) with 4-bromobenzotrifluoride (**2**) was conducted in a mixture consisting 4CzIPN, $NiCl_2$·DME (DME = dimethoxyethane), dtbbpy (4,4'-di-*tert*-butyl-2,2'-dipyridyl), and diisopropylamine (DIPA) in DMF under Ar and white CFL irradiation (Scheme 2a). Interestingly, instead of the desired cross-coupling product (**3**), the dehalogenation product trifluorotoluene (**4**) was obtained in 97% yield (Scheme 2b). Despite the confirmed essential roles of 4CzIPN, light, Ni(II) complex, and DIPA (Table S18, entries 2–6), the presence of a triplet state quencher such as oxygen and 1,1-diphenylethylene shows a limited effect on the reaction yield, which strongly suggests the EnT pathway in inactive (Table S18, entries 8, 9). However, the oxidation product of DIPA was detected by GC-MS (Figure S18), which indicates a photoredox/Ni dual catalytic cycle is likely to yield the dehalogenation product with DIPA as the reductant (see Figure S19 for a proposed reaction mechanism).(29)

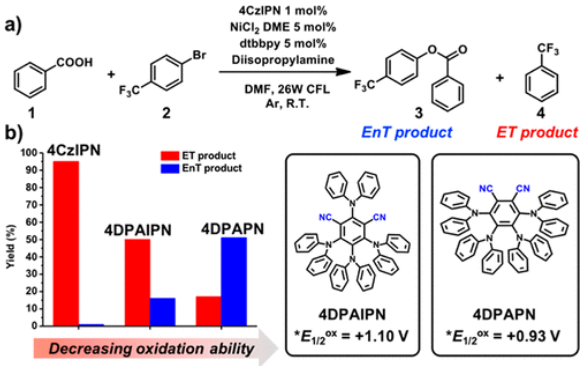

Scheme 2. EnT-Mediated Cross-Coupling of Carboxylic Acids and Aryl Halides

Therefore, in order to achieve the expected cross-coupling product, the oxidation ability of *PC needs to be weakened to suppress the ET event, which can be realized by replacing Cz with a stronger donor, such as diphenylamine (DPA). Indeed, when 4DPAIPN was then used as the PC

(*$E_{1/2}^{ox}$ = +1.10 V(14b)), the yield of product **4** decreased to 57% and the cross-coupling product **3** started to appear (17% yield) (Scheme 2b). The efficiency further increased when the even less oxidative 4DPAPN was used as the PC (*$E_{1/2}^{ox}$ = +0.93 V, Figures S16 and S17), which afforded **3** with 51% yield and only a small amount of **4** (17% yield) (Scheme 2b).(30) The EnT-promoted formation of **3** was further supported by largely diminished product yield under air and triplet quenchers (Table S19, entries 7, 8). It is noteworthy that 4DPAIPN compares favorably to conventional organic photosensitizers such as benzophenone, benzil, 9-flurenone, and common organic dyes such as eosin Y, rhodamine B, and porphyrin (Table S17). After further reaction screening of ligand and Ni(II) salt, an excellent yield (91%) of the cross-coupling product was achieved when sterically hindered amine *N*-isopropyl-*N*-methyl-*tert*-butylamine, a 1:3 molar ratio between carboxylic acid and aryl halide, and solvent *N*,*N*-dimethylacetamide (DMAc) were used (Tables S20–S23). Our result clearly shows that ET proceeds prior to EnT when both pathways are energetically favorable. Therefore, when choosing PC for EnT-promoted reactions, ET has to be suppressed by careful consideration of the electrochemical potentials of all species involved.

4DPAPN gives a wide substrate scope for this reaction (Figure 5). Benzoic acid derivatives with electron-donating or electron-withdrawing substituents can efficiently couple with aryl bromide (**3b**–**3c**, 95% yield). Aliphatic primary, secondary, and tertiary carboxylic acids are highly tolerated (**3d**–**3j**, 79–93% yield). Remarkably, carboxylic acids with a long aliphatic chain (**3g**, 93% yield) or bulky adamantane unit (**3h**, 90% yield) can be delivered to the desired cross-coupling product with excellent yields. Benzyl carboxylic acid can also yield the corresponding ester in good efficiency (**3d**, 79% yield). On the other hand, electron-deficient aryl bromides were able to couple with carboxylic acids smoothly, which is consistent with a previous report.(7b) The reaction tolerated cyanide, carboxylic ester, trifluoromethyl, and halide (**3k**–**3p**, 62–85% yield). Interestingly, a good yield was also obtained despite the presence of an electron-donating group, −OMe (**3m**, 83% yield). *Para*- and *meta*-substitution showed similar coupling efficiency (**3c** and **3n**), while *ortho*-substitution completely hindered the reaction. A heterocycle such as pyridine is also well-tolerated (**3q**, **3r**, 65–83% yield).

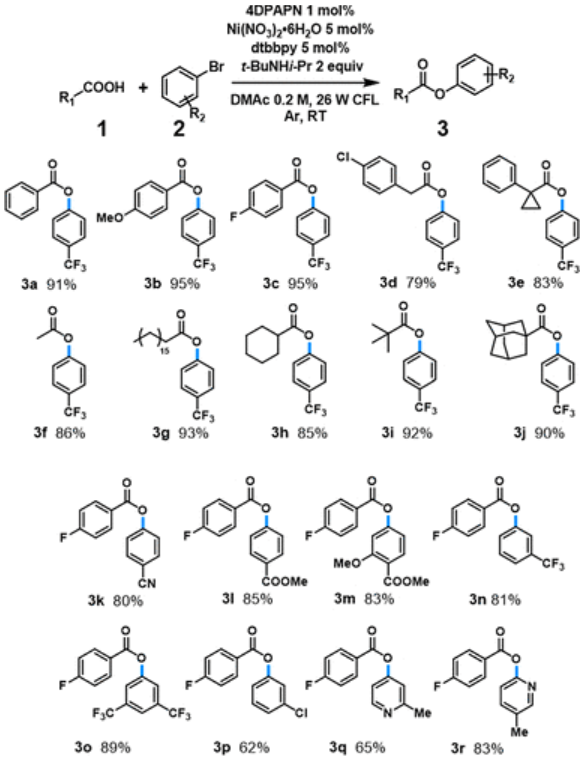

Figure 5. Substrate scope for EnT-mediated cross-coupling of carboxylic acids and aryl halides.

Conclusion

In this study, we use photosensitized *E*/*Z* isomerization of stilbene as a prototypic reaction and demonstrate the importance of the excited state nature of carbazole–cyanobenzene donor–acceptor fluorophores in the energy-transfer-based photocatalytic reactions. A transient absorption spectroscopic study of model compounds 2CzPN and 4CzIPN reveals the coexistence of ^{3}LE and ^{3}CT and their different accessibility for EnT to *E*-stilbene. The advantages of D–A fluorophores as photosensitizers, namely, the tunable ^{3}CT state energy levels, are best realized via ^{3}LE depopulation. Increasing solvent polarity and D–A character are two effective strategies to adjust the energy order between ^{1}CT and ^{3}LE to enhance the accessibility of ^{3}CT for EnT processes. Following this design principle, a new D–A fluorophore, 4DPAPN, that exhibits an appropriate triplet energy is identified to bypass the photoredox process and promote the Ni(II)-catalyzed cross-coupling of carboxylic acids and aryl halides with a wide substrate scope and high selectivity. This work underscores wide applications of D–A fluorophores in EnT-mediated photocatalytic reactions.

The authors declare no competing financial interest.

Acknowledgments

J.Z. acknowledges a National Science Foundation CAREER Award (DMR-1554918) for support of this research. Q.L. thanks the support from China Scholarship Council (201709480009). B.P. and

J.H. acknowledge the support from National Science Foundation (DMR-1654140). S.L. and W.X.S. thank the support from Academic Research Fund Tier 1 (RG2/16). The use of NIR and nanosecond transient absorption spectroscopy at the Center for Nanoscale Materials in Argonne National Laboratory was supported by the U.S. Department of Energy, Office of Science, Office of Basic Energy Sciences, under Award No. DE-AC02-06CH11357. The computational work was partially performed on resources of the National Supercomputing Centre, Singapore (https://www.nscc.sg).

References

1 (a) Schultz, D. M.; Yoon, T. P. *Science* 2014, *343*, 1239176, DOI: 10.1126/science.1239176. (b) Nagib, D. A.; MacMillan, D. W. C. *Nature* 2011, *480*, 224, DOI: 10.1038/nature10647

2 (a) Zeitler, K. *Angew. Chem., Int. Ed.* 2009, *48*, 9785, DOI: 10.1002/anie.200904056. (b) Tucker, J. W.; Stephenson, C. R. *J. Org. Chem.* 2012, *77*, 1617, DOI: 10.1021/jo202538x. (c) Prier, C. K.; Rankic, D. A.; MacMillan, D. W. *Chem. Rev.* 2013, *113*, 5322, DOI: 10.1021/cr300503r

3 Albini, A. *Synthesis* 1981, *1981*, 249, DOI: 10.1055/s-1981-29405

4 (a) Wrighton, M.; Markham, J. *J. Phys. Chem.* 1973, *77*, 3042, DOI: 10.1021/j100644a002. (b) Ikezawa, H.; Kutal, C.; Yasufuku, K.; Yamazaki, H. *J. Am. Chem. Soc.* 1986, *108*, 1589, DOI: 10.1021/ja00267a032

5 (a) Lu, Z.; Yoon, T. P. *Angew. Chem., Int. Ed.* 2012, *51*, 10329, DOI: 10.1002/anie.201204835. (b) Zhao, J.; Brosmer, J. L.; Tang, Q.; Yang, Z.; Houk, K. N.; Diaconescu, P. L.; Kwon, O. *J. Am. Chem. Soc.* 2017, *139*, 9807, DOI: 10.1021/jacs.7b05277. (c) Lei, T.; Zhou, C.; Huang, M. Y.; Zhao, L. M.; Yang, B.; Ye, C.; Xiao, H.; Meng, Q. Y.; Ramamurthy, V.; Tung, C. H.; Wu, L. Z. *Angew. Chem., Int. Ed.* 2017, *56*, 15407, DOI: 10.1002/anie.201708559. (d) Munster, N.; Parker, N. A.; van Dijk, L.; Paton, R. S.; Smith, M. D. *Angew. Chem., Int. Ed.* 2017, *56*, 9468, DOI: 10.1002/anie.201705333. (e) Hormann, F. M.; Chung, T. S.; Rodriguez, E.; Jakob, M.; Bach, T. *Angew. Chem., Int. Ed.* 2018, *57*, 827, DOI: 10.1002/anie.201710441

6 (a) Singh, K.; Staig, S. J.; Weaver, J. D. *J. Am. Chem. Soc.* 2014, *136*, 5275, DOI: 10.1021/ja5019749. (b) Fabry, D. C.; Ronge, M. A.; Rueping, M. *Chem. - Eur. J.* 2015, *21*, 5350, DOI: 10.1002/chem.201406653. (c) Singh, A.; Fennell, C. J.; Weaver, J. D. *Chem. Sci.* 2016, *7*, 6796, DOI: 10.1039/C6SC02422J

7 (a) Heitz, D. R.; Tellis, J. C.; Molander, G. A. *J. Am. Chem. Soc.* 2016, *138*, 12715, DOI: 10.1021/jacs.6b04789. (b) Welin, E. R.; Le, C.; Arias-Rotondo, D. M.; McCusker, J. K.; MacMillan, D. W. *Science* 2017, *355*, 380, DOI: 10.1126/science.aal2490

8 Blum, T. R.; Miller, Z. D.; Bates, D. M.; Guzei, I. A.; Yoon, T. P. *Science* 2016, *354*, 1391, DOI: 10.1126/science.aai8228

9 Troster, A.; Alonso, R.; Bauer, A.; Bach, T. *J. Am. Chem. Soc.* 2016, *138*, 7808, DOI: 10.1021/jacs.6b03221

10 (a) Juris, A.; Balzani, V.; Barigelletti, F.; Campagna, S.; Belser, P.; von Zelewsky, A. *Coord. Chem. Rev.* 1988, *84*, 85, DOI: 10.1016/0010-8545(88)80032-8. (b) Larsen, C. B.; Wenger, O. S. *Chem. - Eur. J.* 2018, *24*, 2039, DOI: 10.1002/chem.201703602

11 Romero, N. A.; Nicewicz, D. A. *Chem. Rev.* 2016, *116*, 10075, DOI: 10.1021/acs.chemrev.6b00057

12 Zhao, J.; Wu, W.; Sun, J.; Guo, S. *Chem. Soc. Rev.* 2013, *42*, 5323, DOI: 10.1039/c3cs35531d

13 (a) Arceo, E.; Montroni, E.; Melchiorre, P. *Angew. Chem., Int. Ed.* 2014, *53*, 12064, DOI: 10.1002/anie.201406450. (b) Alonso, R.; Bach, T. *Angew. Chem., Int. Ed.* 2014, *53*, 4368, DOI: 10.1002/anie.201310997. (c) Mojr, V.; Svobodova, E.; Strakova, K.; Nevesely, T.; Chudoba, J.; Dvorakova, H.; Cibulka, R. *Chem. Commun.* 2015, *51*, 12036, DOI: 10.1039/C5CC01344E. (d) Metternich, J. B.; Gilmour, R. *J. Am. Chem. Soc.* 2015, *137*, 11254, DOI: 10.1021/jacs.5b07136. (e) Cai, W.; Fan, H.; Ding, D.; Zhang, Y.; Wang, W. *Chem. Commun.* 2017, *53*, 12918, DOI: 10.1039/C7CC07984B

14 (a) Lu, J.; Khetrapal, N. S.; Johnson, J. A.; Zeng, X. C.; Zhang, J. *J. Am. Chem. Soc.* 2016, *138*, 15805, DOI: 10.1021/jacs.6b08620 . (b) Luo, J.; Zhang, J. *ACS Catal.* 2016, *6*, 873, DOI: 10.1021/acscatal.5b02204. (c) Luo, J.; Zhang, J. *J. Org. Chem.* 2016, *81*, 9131, DOI: 10.1021/acs.joc.6b01704. (d) Luo, J.; Zhang, X.; Lu, J.; Zhang, J. *ACS Catal.* 2017, *7*, 5062, DOI: 10.1021/acscatal.7b01010

15 (a) Uoyama, H.; Goushi, K.; Shizu, K.; Nomura, H.; Adachi, C. *Nature* 2012, *492*, 234, DOI: 10.1038/nature11687. (b) Kabe, R.; Adachi, C. *Nature* 2017, *550*, 384, DOI: 10.1038/nature24010

16 Dias, F. B.; Santos, J.; Graves, D. R.; Data, P.; Nobuyasu, R. S.; Fox, M. A.; Batsanov, A. S.; Palmeira, T.; Berberan-Santos, M. N.; Bryce, M. R.; Monkman, A. P. *Adv. Sci.* 2016, *3*, 1600080, DOI: 10.1002/advs.201600080

17 Samanta, P. K.; Kim, D.; Coropceanu, V.; Bredas, J. L. *J. Am. Chem. Soc.* 2017, *139*, 4042, DOI: 10.1021/jacs.6b12124

18 Baryshnikov, G.; Minaev, B.; Agren, H. *Chem. Rev.* 2017, *117*, 6500, DOI: 10.1021/acs.chemrev.7b00060

19 (a) Penfold, T. J.; Gindensperger, E.; Daniel, C.; Marian, C. M. *Chem. Rev.* 2018, *118*, 6975, DOI: 10.1021/acs.chemrev.7b00617. (b) Penfold, T. J.; Dias, F. B.; Monkman, A. P. *Chem. Commun.* 2018, *54*, 3926, DOI: 10.1039/C7CC09612G

20 (a) Ishimatsu, R.; Matsunami, S.; Shizu, K.; Adachi, C.; Nakano, K.; Imato, T. *J. Phys. Chem. A* 2013, *117*, 5607, DOI: 10.1021/jp404120s. (b) Ishimatsu, R.; Edura, T.; Adachi, C.; Nakano, K.; Imato, T. *Chem. - Eur. J.* 2016, *22*, 4889, DOI: 10.1002/chem.201600077

21 Saltiel, J.; Hammond, G. S. *J. Am. Chem. Soc.* 1963, *85*, 2515, DOI: 10.1021/ja00899a036

22 Herkstroeter, W. G.; McClure, D. S. *J. Am. Chem. Soc.* 1968, *90*, 4522, DOI: 10.1021/ja01019a002

23 Hosokai, T.; Matsuzaki, H.; Nakanotani, H.; Tokumaru, K.; Tsutsui, T.; Furube, A.; Nasu, K.; Nomura, H.; Yahiro, M.; Adachi, C. *Sci. Adv.* 2017, *3*, e1603282, DOI: 10.1126/sciadv.1603282

24 Chan, C.-Y.; Cui, L.-S.; Kim, J. U.; Nakanotani, H.; Adachi, C. *Adv. Funct. Mater.* 2018, *28*, 1706023, DOI: 10.1002/adfm.201706023

25 Based on the ET value of 2CzPN (2.63 eV). The difference is estimated from the reported values from Zhang, D.; Duan, L. SPIE Newsroom 2017, DOI: 10.1117/2.1201611.006797 .

26 Crosby, P. M.; Dyke, J. M.; Metcalfe, J.; Rest, A. J.; Salisbury, K.; Sodeau, J. R. *J. Chem. Soc., Perkin Trans. 2* 1977, *2*, 182, DOI: 10.1039/p29770000182

27 Hammond, G. S.; Saltiel, J.; Lamola, A. A.; Turro, N. J.; Bradshaw, J. S.; Cowan, D. O.; Counsell, R. C.; Vogt, V.; Dalton, C. *J. Am. Chem. Soc.* 1964, *86*, 3197, DOI: 10.1021/ja01070a002

28 Lowry, M. S.; Goldsmith, J. I.; Slinker, J. D.; Rohl, R.; Pascal, R. A.; Malliaras, G. G.; Bernhard, S. *Chem. Mater.* 2005, *17*, 5712, DOI: 10.1021/cm051312+

29 Corcoran, E. B.; Pirnot, M. T.; Lin, S.; Dreher, S. D.; DiRocco, D. A.; Davies, I. W.; Buchwald, S. L.; MacMillan, D. W. *Science* 2016, *353*, 279, DOI: 10.1126/science.aag0209

30 Both 4DPAIPN and 4DPAPN can efficiently catalyze the *E*/*Z* isomerization of stibene, yielding a *Z*/*E* ratio of 8.4 and 11.1, respectively. These ratios are higher than the corresponding Cz-substituted version, which is consistent with the increasing D–A character when a stronger donor DPA is used.

Supporting Information

The Supporting Information is available free of charge on the ACS Publications website at DOI: 10.1021/jacs.8b07271.

Materials and methods, synthesis and characterization of D–A fluorophores, photocatalytic reaction procedures, computational results, transient absorption spectroscopy, and NMR spectra (PDF)

pdf

ja8b07271_si_001.pdf (5.8 MB)